Faculty for mechanical engineering
MathCCES
Prof. Dr. Manuel Torrilhon

Seminar report

Towards weakly compressible flows

Jannick Wolters
Matriculation number: 302517

July 2016

Contents

Chapter 1

Introduction

The classical approach to solving computational fluid dynamics (CFD) breaks down to two different approaches.
It usually comes down to the role which the density plays in a given system. For slow flow speeds, as they are occurring e.g. in the automotive industry, the air that is interacting with the car can be considered constant w.r.t its density. Compression effects are too weak at these speeds to have an impact on the overall flow behavior. In such fields the model used for a computation would be the 'incompressible Navier-Stokes equations'.
These equations derive from the fully compressible Navier-Stokes equations, which on the other hand can be used to model a variable density as for example needed in aerospace engineering. Here flow phenomena are heavily depending on density changes (e.g. shocks in supersonic flight) and thus must be taken into account.
As it will be shown the two equation sets differ in their mathematical nature and therefore can not be solved with the same approaches. This results in two different validity regimes which can be seen in figure 1.1. The compressible Navier-Stokes equations are valid up to a Mach number of $Ma \approx 0.3$, whereas the compressible equations are valid on the whole domain but struggle in the zero Mach number limit and are much more expensive on the computational side.

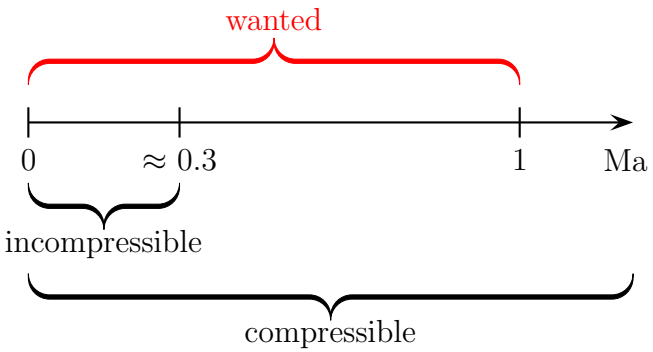

Figure 1.1: Validity regime of the Navier-Stokes equations

Even though the complete Mach number domain appears to be covered, some applications fit right in between the two use cases. These applications have flow speeds too high for the incompressible equations, but never reach the transonic or even the supersonic domain and thus it might not be worth it (computational wise) to solve for the compressible Navier-Stokes equations. Such problems might be temperature driven flows as they occur in chemical reactions. The core research papers that have been reviewed for this report will use the same approach to derive a suitable system of 'weakly compressible' equations, but will further describe different approaches to deal with the derived set of equations.

Chapter 2

Multi-scale expansion

To get from the well known compressible Navier-Stokes equations to the weakly compressible equations, an asymptotic analysis on the dimensionless compressible equations will be performed according to [Mun+03] .
Assuming the equations are closed by the ideal gas law

$$p = \rho RT = (\gamma - 1)\rho\epsilon \tag{2.1}$$

one can write the equations in its primitive variables (ρ, U, p), instead of the conserved form $(\rho, \rho v, e)$, which is more commonly used.

$$\rho_t + \nabla \cdot (\rho v) = 0 \tag{2.2}$$

$$v_t + (v \cdot \nabla)v + \frac{1}{M^2\rho}\nabla p = \frac{1}{Re\rho}\Delta v + \frac{1}{3Re\rho}\nabla(\nabla \cdot v) + \frac{1}{Fr^2}g \tag{2.3}$$

$$p_t + v \cdot \nabla p + \gamma p \nabla \cdot v = \frac{\gamma}{PrRe}\Delta T \tag{2.4}$$

with the non-dimensional quantities the Mach number $M = v_{ref}/\sqrt{p_{ref}/\rho_{ref}} = v_{ref}/c_{ref}$, the Reynolds number $Re = x_{ref}\rho_{ref}v_{ref}/\mu$, the Prandtl number $Pr = \mu c_p/\lambda$ and the Froude number $Fr = \sqrt{v_{ref}^2/g_{ref}x_{ref}}$. Here especially the Mach number is of interest. When dealing with a fully compressible flow regime the reference velocity u_{ref} and speed of sound c_{ref} are chosen equally. For an almost incompressible fluid, this choice is inappropriate, as flow velocity and the speed of sound differ by multiple orders of magnitude, with the speed of sound being much higher. The reference value for the speed of

sound therefore has to be chosen independently of the reference value for the flow velocity. This can be done by choosing a suitable reference pressure, e.g. $p_{ref} = p_{mean}$.
As the Mach number is a parameter in the dimensionless equations above and the flow variables therefore depend on it, an asymptotic expansion of the general form

$$f(x,t;M) = f^{(0)}(g(x,t,M)) + Mf^{(1)}(g(x,t,M)) + M^2 f^{(2)}(g(x,t,M)) + \mathcal{O}(M^2) \tag{2.5}$$

can be performed. For example an expansion on the pressure p yields

$$p = p^{(0)} + Mp^{(1)} + M^2 p^{(2)} \tag{2.6}$$

This expansion can be applied to each flow variable to analyze its asymptotic behavior.
The general idea behind this approach is to obtain a closed system of equations of leading order, which can be solved more easily while maintaining the solution in a approximative sense. Applying the obtained approximation to the first order equations, which also form a closed system that takes the leading order solution as an input, yields a further improvement. This procedure can be continued with all higher order equations.
With $(g(x,t,M)) = (x, \xi = Mx, t)$ the transformation is called a multi scale expansion, because it has a single time scale t and two spatial scales, a slow (x) and a fast one (ξ) moving with the Mach number. Spatial derivatives thereby become $\nabla f = \nabla_x f + M\nabla_\xi f$.
Applying the expansion to the Navier-Stokes system unfortunately is impossible as no closed system of equations can be found for any order. The only closed system that can be found is the one with leading order velocity, density and pressure together with second order pressure terms. The different pressure orders therefore seem to have different functions in the system. An investigation yields:

- $p^{(0)}$ thermodynamic pressure: constant in the zero Mach number limit and fulfills the equation of state
- $p^{(1)}$ acoustic pressure: fulfills linear acoustic equations (ξ-scale), but is constant on the slow scale and therefore no quantity of interest for low Mach number flows

- $p^{(2)}$ hydrodynamic pressure: acts as a Lagrange multiplier w.r.t the divergence free constraint in the incompressible limit; even though the constraint is defined by the thermodynamic pressure, it is fulfilled by the hydrodynamic pressure

All in all in the limit of $M \to 0$ the equations converge to:

$$\rho_t^{(0)} + \nabla_x(\rho^{(0)} v^{(0)}) + = 0 \tag{2.7}$$

$$v_t^{(0)} + (v^{(0)} \cdot \nabla_x) v^{(0)} + \frac{1}{\rho^{(0)}} \nabla_x p^{(2)} = \frac{1}{Re \rho^{(0)}} \Delta_{xx} v^{(0)} + \frac{1}{Fr^2} g \tag{2.8}$$

$$\nabla_x \cdot v^{(0)} = -\frac{p_t^{(0)}}{\gamma p^{(0)}} \tag{2.9}$$

$$p_t^{(0)} = -\frac{\gamma p^{(0)}}{|V|} \int_{\partial V} v^{(0)} \cdot n ds \tag{2.10}$$

This system is now called the system of incompressible Navier-Stokes equations with a variable density. This set of equations can now be used to derive schemes for the different problem sets. Here it should be noticed that the energy equation was omitted in the derivation, but will be added in later discussions. A derivation including the equation can also be done as stated in [Mun+03].

Chapter 3

Application to temperature driven problems

Flows in which density changes are induced by a temperature gradient, such as chemical reactions, can be characterized by low-Mach-number speeds and a hydrodynamical incompressible behavior [Ran00]. They therefore fit the derived set of equations from the previous chapter.

3.1 Derivation

For the case of stationary flow the time derivatives drop out of the previously derived system

$$\nabla_x \cdot (\rho^{(0)} v^{(0)}) = 0 \tag{3.1}$$

$$(v^{(0)} \cdot \nabla_x) v^{(0)} + \frac{1}{\rho^{(0)}} \nabla_x p^{(2)} = \frac{1}{Re \rho^{(0)}} \Delta_{xx} v^{(0)} + \frac{1}{Fr^2} g \tag{3.2}$$

Heat transfer has been neglected in the above considerations, but it can be shown that in principle the equations can treat heat transfer as well. The stationary energy equation reads:

$$c_p \rho v \cdot \nabla T - \nabla \cdot (\lambda \nabla T) = h_{ext} \tag{3.3}$$

It is important to note that specific heat capacity $c_p = c_p(T)$ and the viscosity $\mu = \mu(T)$ are assumed to be functions of the temperature. Furthermore equation 3.1 can be rewritten in case of single species flow, yielding:

$$\nabla \cdot v - \frac{1}{T} v \cdot \nabla T = 0 \tag{3.4}$$

Now the systems primal variables are $u = \{p_{hyd}, v, T\}$. Therefore the mass equation is used for the computation of the velocity v, whereas the momentum equation is used to compute the hydrodynamic pressure $p^{(2)}$.
As the density is obviously not a primal variable, it has to be obtained by material laws. In this case again the ideal gas law is used:

$$\rho = \frac{p^{(0)}\mathcal{M}}{RT} \tag{3.5}$$

$p^{(0)}$ in this context is supposed to be know a priori, see [BR99] for further information.
The system is closed by imposing appropriate boundary conditions:

$$v_{|\Gamma_{rigid}} = 0, \quad v_{|\Gamma_{in}} = v_{in}, \quad \mu\partial_n v + pn_{|\Gamma_{out}} = 0, \quad T_{|\partial\Omega} = 0 \tag{3.6}$$

For the general application on chemical reactions, further equations for species concentrations and potentially nonlinear source terms representing the reactions themselves would be needed. Nevertheless the case treated in [Ran00] is restricted to temperature variations solely depending on external source terms.

3.2 Discretization

To discretize the system of equations in a finite element sense, the equations will at first be rewritten in variational form:

$$(\nabla \cdot v, \phi) - (T^{-1}v \cdot \nabla T, \phi) = 0 \qquad \forall \phi \in L^2_0(\Omega) \tag{3.7}$$

$$(\rho v \cdot \nabla v, \chi) + (\mu \nabla v, \nabla \chi) - (p, \nabla \cdot \chi) = (\rho f_{ext}, \chi) \qquad \forall \chi \in H^1_0(\Omega)^d \tag{3.8}$$

$$(c_p \rho v \cdot \nabla T, \psi) + (\lambda \nabla T, \psi) = (h_{ext}, \psi) \qquad \forall \psi \in H^1_0(\Omega) \tag{3.9}$$

reducing the infinite dimensional function spaces to discrete finite dimensional spaces, denoted by the subscript h, yields then:

$$(\nabla \cdot v_h, \phi_h) - (T_h^{-1}v \cdot \nabla T_h, \phi_h) = 0 \qquad \forall \phi_h \in L^2_{0,h}(\Omega) \tag{3.10}$$

$$(\rho v_h \cdot \nabla v_h, \chi_h) + (\mu \nabla v_h, \nabla \chi_h) - (p_h, \nabla \cdot \chi_h) = (\rho f_{ext}, \chi_h) \quad \forall \chi_h \in H^1_{0,h}(\Omega)^d \tag{3.11}$$

$$(c_p \rho v_h \cdot \nabla T_h, \psi_h) + (\lambda \nabla T_h, \psi_h) = (h_{ext}, \psi_h) \qquad \forall \psi_h \in H^1_{0,h}(\Omega) \tag{3.12}$$

or rather in a more compact form written as the system:

$$A(u_h; \varphi_h) = F(\varphi) \qquad \forall \varphi_h \in V_h \tag{3.13}$$

with $u = \{p, v, T\}$, $\varphi = \phi, \chi, \psi$ and the semi-linear form

$$\begin{aligned} A(u; \varphi) := (\nabla \cdot v_h, \phi_h) - (T_h^{-1} v_h \cdot \nabla T_h, \phi_h) + (\rho v_h \cdot \nabla v_h, \chi_h) + (\mu \nabla v_h, \nabla \chi_h) \\ -(p_h, \nabla \cdot \chi_h) + (\rho c_p v_h \cdot \nabla T_h, \psi_h) + (\lambda \nabla T_h, \nabla \psi_h) \end{aligned} \tag{3.14}$$

and the linear form

$$F(\varphi_h) = (\rho f_{ext}, \chi_h) + (h, \psi_h) \tag{3.15}$$

The main problem in dealing with these equations is the stiffness of the velocity-pressure coupling. To deal with the stiff coupling a least-squares stabilization for the pressure term and streamline diffusion for the transport terms is applied to the system in 3.13. This results in an augmented system

$$A_h(u_h; \varphi_h) = F_h(\varphi) \qquad \forall \varphi_h \in V_h \tag{3.16}$$

with $A_h(\cdot;\cdot) \coloneqq A(\cdot;\cdot) + s_h(\cdot,\cdot)$ and $F_h(\cdot) \coloneqq F(\cdot) + r_h(\cdot)$. The added terms assemble from summation of the individual stabilization terms. The pressure least-square stabilization yields:

$$s_h^p(u_h, \phi_h) = \sum_{K \in T_h} \alpha_K (\bar{v}_h \cdot \nabla v_h - \nabla \cdot [\mu \nabla v_h] + \nabla p_h, \nabla \phi_h)_K \tag{3.17}$$

$$r_h^p(u_h, \phi_h) = \sum_{K \in T_h} \alpha_K (\rho f, \nabla \phi_h)_K \tag{3.18}$$

Whereas streamline diffusion is applied for the velocity v:

$$s_h^v(u_h, \chi_h) = \sum_{K \in T_h} \delta_K (\rho \bar{v}_h \cdot \nabla v_h - \nabla \cdot [\mu \nabla v_h] + \nabla p_h, \rho \bar{v}_h \cdot \nabla \chi_h)_K \tag{3.19}$$

$$r_h^v(u_h, \chi_h) = \sum_{K \in T_h} \delta_K (\rho f, \rho \bar{v}_h \cdot \nabla \chi_h)_K \tag{3.20}$$

and the temperature T:

$$s_h^T(u_h, \psi_h, \phi_h) = \sum_{K \in T_h} \gamma_K(\rho c_p \bar{v}_h \cdot \nabla T_h - \nabla \cdot [\lambda \nabla T_h], \rho c_p \bar{v}_h \cdot \nabla \psi_h)_K \quad (3.21)$$

$$r_h^T(u_h, \psi_h, \phi_h) = \sum_{K \in T_h} \gamma_K(h, \rho c_p \bar{v}_h \cdot \nabla \psi_h)_K \quad (3.22)$$

with $\bar{v}_h$ being an approximation to the current velocity field for example from a previous iteration. The general idea behind streamline diffusion is to add an artificial diffusion term only in the direction of the streamlines and thus improving robustness while maintaining correct flow behavior. It is an open question how much diffusion should be added to fulfill these properties. See [Bra98] for further discussion.
The now obtained augmented system can be solved by a defect-correction iteration as it is commonly used for the incompressible equations. In general the algorithm does the following:

1. freeze nonlinear coefficients from the previous iteration u_h^{i-1}
2. solve the now linearized system of equations for the correction term δu_h^i using also the defects from the previous iteration
3. update the solution vector (optional: apply relaxation to improve robustness) and the density according to the equation of state
4. check for convergence criterion, otherwise continue with the next iteration

3.3 Numerical results

The following results presented have been obtained by [Bra98]. The problem that is considered consists of a methane burner, where a mixture of methane (CH_4) and air (mainly N_2 and O_2) flows from the bottom to the top of the burner. On the way it will pass a couple of heated slots, which will ultimately lead to the ignition of the mixture (see figure 3.1).

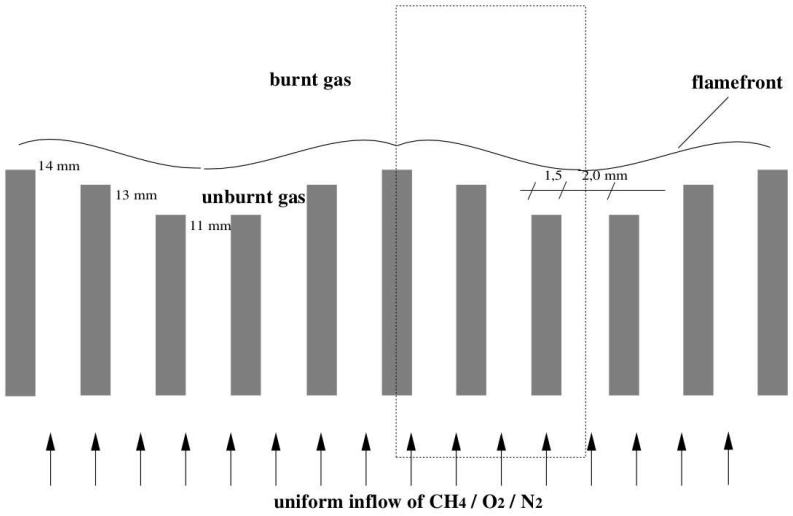

Figure 3.1: Geometry of the methane burner; from [Bra98]

The slots vary in height from 11mm to 14mm while having a uniform spacing of 2mm. The inflow velocity is set to be 0.2m/s across the inlet but will accelerate up to 1m/s due to the heated slots. A slot temperature of 2000 K is set in order to achieve ignition.
A reaction mechanism with 15 species and 84 elementary reactions is implemented to correctly describe the burning process.
On the computational side a quadrilateral adaptive mesh is used, starting at 1344 cells in the coarsest configuration and around 5000 cells on average during calculations. To make use of the problems symmetry, only 3 slots have actively been calculated.
The obtained results are shown in figure 3.2.

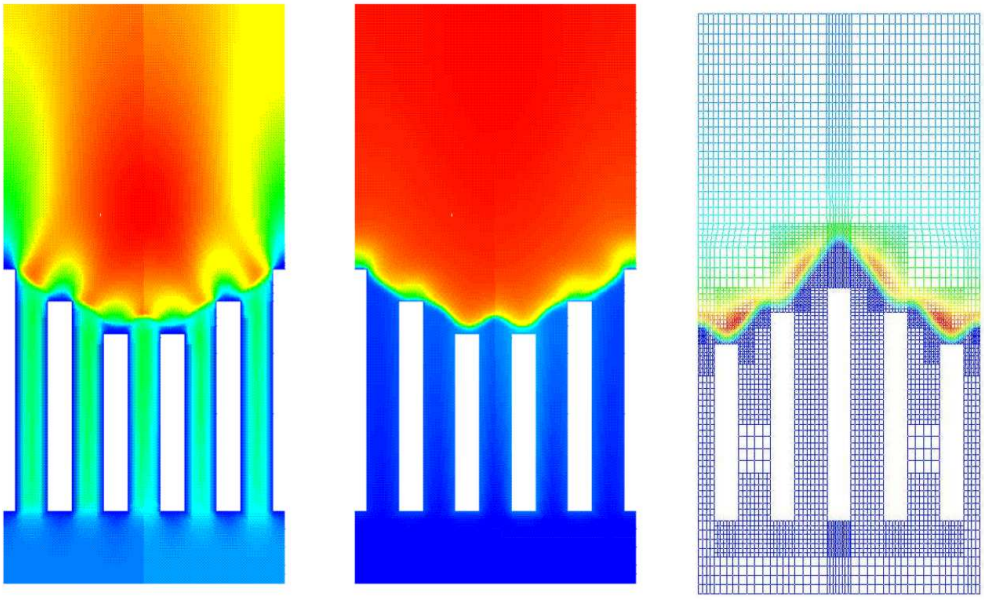

Figure 3.2: Simulation results: velocity (left), temperature (middle), mesh with 5000 cells (right); from [Bra98]

It is clearly visible that the flame front is located above the heated slots, which is expected as the slots exit flow speed is higher than the flame speed of methane. Lowering the inlet speed would result in extinguishing the flame, as the flame front would lower below the slot top and thus not enough heat being transfered to trigger the ignition.

Chapter 4

Multi-Pressure-Variable scheme

The Multi-Pressure-Variable scheme takes the results from chapter 2 and tries to construct a solver valid for the whole subsonic domain. This is all done according to [Mun+03].

4.1 Derivation

The asymptotic equations derived in chapter 2 are only viable for a limited range of small Mach number flows. To construct a scheme from the fully compressible Navier-Stokes equations, two additional equations are required to close the system. The first equation can be derived from equation 2.6 by interpreting the analysis done above. Thus can the pressure $p^{(2)}$ be interpreted as a rescaling of the total pressure p using the known values of $p^{(0)}$ and $p^{(1)}$. To be able to extend the schemes ability, in terms of higher Mach numbers, beyond the limitations of the asymptotic analysis, the asymptotic equations are used as a predictor and the fully compressible equations as a corrector step. This pretty much extends the solvability to the complete subsonic domain. To be able to do this, consistency between the total pressure and all the terms from the asymptotic analysis has to be given at any iteration The decomposition uses the previously discussed observations, as $p^{(0)}$ becomes constant in space and $p^{(1)}$ constant on the small flow scale in the incompressible limit. $p^{(0)}$ and $p^{(1)}$ can therefore be written as:

$$p^{(0)} := \frac{1}{|V|} \int_V p dx \tag{4.1}$$

and

$$p^{(1)} := \frac{1}{M|V_{ac}|}\int_{V_{ac}} p - p^{(0)}dx \tag{4.2}$$

From consistency follows furthermore:

$$p^{(2)} := \frac{1}{M^2}(p - p^{(0)} - Mp^{(1)}) \tag{4.3}$$

Evolution in time for $p^{(0)}$ and $p^{(1)}$ are calculated by the asymptotic equations. Meaning $p^{(0)}$ is determined by compression or heat transfer from the boundaries:

$$p_t^{(0)} = -\frac{\gamma p^{(0)}}{|V|}\int_{\partial V} v \cdot nds + \frac{\gamma}{PrRe|V|}\int_{\partial V} \nabla_x T \cdot nds \tag{4.4}$$

Without any prescribed external forces $p^{(0)}$ will therefore become constant in time.
To calculate the temporal change in $p^{(1)}$, a linear acoustic system has to be solved:

$$p_t^{(1)} + \gamma p^{(0)}\nabla_\xi \bar{v} = 0 \tag{4.5}$$

$$\bar{v}_t + \frac{1}{\bar{\rho}}\nabla_\xi p^{(1)} = -\frac{\overline{(\tilde{\rho}\tilde{v})_t}}{\bar{\rho}} \tag{4.6}$$

where $\bar{\rho}$ and $\bar{v}$ represent the long wavelength contributions defined by:

$$\bar{\rho} := \frac{1}{|V_{ac}|}\int_{V_{ac}} \rho dx \tag{4.7}$$

and

$$\bar{v} := \frac{1}{|V_{ac}|}\int_{V_{ac}} v dx \tag{4.8}$$

Note that the singularity at $M = 0$ has here been removed by approximating

$$\frac{1}{M^2}\nabla p \approx -(\overline{\rho v})_t + \nabla p^{(2)} \tag{4.9}$$

as the thermodynamic pressure $p^{(0)}$ is constant in space and thus $\nabla p^{(0)} = 0$. $\nabla p^{(1)}$ act on the large scale of acoustics and therefore leads to a temporal change of the momentum average $-(\overline{\rho v})_t$.

This results in the following Multiple Pressure Variable (MPV) scheme given as (in primitive variables):

$$\rho_t^{(0)} + \nabla(\rho^{(0)} v^{(0)}) + = 0 \tag{4.10}$$

$$v_t + (v \cdot \nabla)v + \frac{1}{\rho}\nabla p^{(2)} = -\frac{1}{M\rho}\nabla p^{(1)} + \frac{1}{Re\rho}\Delta v + \frac{1}{3Re\rho}\nabla(\nabla \cdot v) + \frac{1}{Fr^2}g \tag{4.11}$$

$$\begin{aligned} M^2 p_t^{(2)} + M^2 v \cdot \nabla p^{(2)} + M^2 \gamma p^{(2)} \nabla \cdot v = -p_t^{(0)} - M p_t^{(1)} - M v \cdot \nabla p^{(1)} \\ -\gamma(p^{(0)} + M p^{(1)})\nabla \cdot v + \frac{\gamma}{PrRe}\Delta T \end{aligned} \tag{4.12}$$

The advantage on this scheme is that it converges to a standard incompressible scheme in the limit $M \to 0$ [Kle+01] or to a standard Godunov scheme for $M \to 1$ [Ger98]. Even recoupling of acoustic phenomena is possible (important in e.g. reaction chambers).
To solve this system, a convection-diffusion splitting is most likely to succeed, but in general any numerical scheme can be applied.

4.2 Numerical results

The presented results are taken from [Rol+05]. Here the MPV-scheme was solved using convection-diffusion splitting. The convection terms can thus be solved explicitly, while the diffusion terms are treated implicitly. This improves performance as treating the diffusion terms explicitly would lead to small time steps due to the CFL-restriction. If applied to the MPV-scheme, only the flow velocity is included in the explicit step, while all acoustic phenomena are being treated implicitly.
The simulated test case is the well known lid driven cavity case with a Reynolds number of $Re = 1000$, Prandtl number of $Pr = 0.7$ and a Mach number of $Ma = 0.0005$. The left boundary wall temperature is set to 293.6 K, while the right wall is set to 293.6 K + ΔT. For ΔT being small, the density can be assumed as constant and thus an incompressible Boussinesq approach would be valid. If ΔT is no longer small, this is no longer the case and to show this the results in figure 4.1 are based on $\Delta T = 150$ K.

FIGURE 1. Streamline visualization of the lid driven cavity flow at Re = 1000.

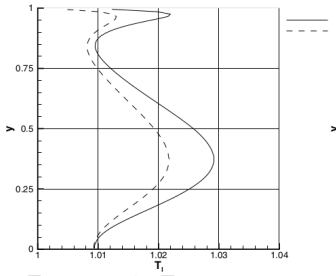

FIGURE 2. Temperatures at the left (cold) walls.

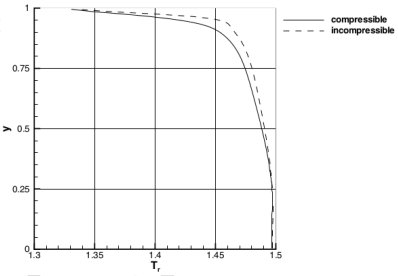

FIGURE 3. Temperatures at the right (hot) walls.

Figure 4.1: Simulation results from [Rol+05]

The most differences in the obtained results are found at the boundary layer. The incompressible calculation can not account for the temperature driven density changes and this results in thicker thermal boundary layer compared to the MPV-scheme. The relative L_2 errors from the two simulations (compressible and incompressible Boussinesq) on both walls can be taken from figure 4.2.

Table 1
Relative L_2 error of density and temperature at the left wall

ΔT (K)	30	60	90	120	150
ρ (%)	4.4	8.3	12	15	18

Table 2
Relative L_2 error of density and temperature at the right wall

ΔT (K)	30	60	90	120	150
ρ (%)	4	7.6	11	14	16

Figure 4.2: L_2 error at the left and right boundary; from [Rol+05]

Chapter 5

Summary

The gathered information about the derivation of weakly compressible flow models resulted in a better understanding of the Navier-Stokes equations. The asymptotic expansion of the pressure revealed the roles which the different pressure orders take in the system and how they are influencing the overall flow behavior. Two different approaches to the asymptotic equations have then been highlighted and each could show, that it better suited for its purpose than the classical incompressible and fully compressible versions of the Navier-Stokes equations. While the method introduced by [Ran00] is closer to the incompressible case in terms of numerical treatment, the MPV-scheme by [Mun+03] appears to be more universal and straight forward in the application. In the case of modeling chemical reactions, it has already been shown that those can be treated with the more classical weakly compressible scheme [Bra98]. Comparable results could not be found for the MPV-scheme.
As the performance of both schemes appears to be quite evenly matched, it comes down to the problem itself and maybe already existing code structures, which one is to use.

Bibliography

[Bra98] Malte Braack. "An adaptive finite element method for reactive flow problems". PhD thesis. IWR, 1998.

[BR99] Malte Braack and Rolf Rannacher. *Adaptive finite element methods for low Mach number flows with chemical reactions*. Citeseer, 1999.

[Ger98] Karl Josef Geratz. *Erweiterung eines Godunov-Typ-Verfahrens für zwei-dimensionale kompressible Strömungen auf die Fälle kleiner und verschwindender Machzahl*. Shaker, 1998.

[Kle+01] Rupert Klein et al. "Asymptotic adaptive methods for multi-scale problems in fluid mechanics". In: *Practical Asymptotics*. Springer, 2001, pp. 261–343.

[Mun+03] C-D Munz et al. "The extension of incompressible flow solvers to the weakly compressible regime". In: *Computers & Fluids* 32.2 (2003), pp. 173–196.

[Ran00] Rolf Rannacher. "Finite element methods for the incompressible Navier-Stokes equations". In: *Fundamental directions in mathematical fluid mechanics*. Springer, 2000, pp. 191–293.

[Rol+05] Sabine Roller et al. "Calculation of low Mach number acoustics: a comparison of MPV, EIF and linearized Euler equations". In: *ESAIM: Mathematical Modelling and Numerical Analysis* 39.3 (2005), pp. 561–576.